Recent Results of the Hadron Resonance Gas Model and the Chemical Freeze-out of Strange Hadrons

K. A. Bugaev[1*], A. I. Ivanytskyi[1], D. R. Oliinychenko[1,2], E. G. Nikonov[3], V. V. Sagun[1] and G. M. Zinovjev[1]

[1] *Bogolyubov Institute for Theoretical Physics, Metrologichna str. 14^B, Kiev 03680, Ukraine*
[2] *FIAS, Goethe-University, Ruth-Moufang Str. 1, 60438 Frankfurt upon Main, Germany*
[3] *Laboratory for Information Technologies, JINR, Joliot-Curie str. 6, 141980 Dubna, Russia*
$*$ *E-mail: Bugaev@th.physik.uni-frankfurt.de*

arXiv:1412.6571v2 [hep-ph] 24 Jan 2015

Abstract

A detailed discussion of recent results obtained within the hadron resonance gas model with the multi-component hard core repulsion is presented. Among them there are the adiabatic chemical freeze-out criterion, the concept of separate chemical freeze-out of strange particles and the effects of enhancement and sharpening of wide resonances and quark gluon bags occurring in a thermal medium. These findings are discussed in order to strengthen the planned heavy-ion collision experimental programs at low collision energies. We argue, that due to found effects, at the center of mass collision energy 4-8 GeV the quark gluon bags may appear directly or in decays as new heavy resonances with the narrow width of about 50-150 MeV and with the mass above 2.5 GeV.

1. Basic elements of the hadron resonance gas model. The recent findings [1, 2, 3] obtained by the hadron resonance gas model (HRGM) resolved a few old puzzles on the chemical freeze-out and gave a novel look at some old problems of QCD phenomenology. One of the most successful version of the HRGM, the HRGM1, was developed in [5, 6]. The novel version of this model, the HRGM2, which was worked out in [1, 2], has the same basic properties as the HRGM1, namely, it employes the hard-core repulsion between the hadrons, it includes all hadronic resonances with masses up to 2.5 GeV with their finite width. Also it accounts both the thermal hadronic multiplicities and the nonthermal ones which are coming from the decay of heavy resonances. Finally, the HRGM2 explicitly accounts for the strangeness conservation by finding out the chemical potential of the strange charge from a condition of vanishing strangeness. Despite slightly different particle tables employed in the HRGM1 and HRGM2 and a systematic accounting for the resonance width in HRGM2, these models give very similar results for the chemical freeze out (FO) parameters for the same values of the hadronic hard-core radii [1]. This is shown in Fig. 1 for the same hadronic hard-core radii $R = 0.3$ fm.

2. Adiabatic chemical FO criterion and effective hadronic mass spectrum. A thorough investigation of the traditional chemical FO criteria performed in [1] for the HRGM1 and HRGM2 gave rather valuable results. Although the discussion about the reliable chemical FO criterion has a long history [5, 7], only very recently it was demonstrated that none of the previously suggested chemical FO criteria, including the most popular one of constant energy per particle $E/N \simeq 1.1$ GeV [8, 9] and the criterion of constant entropy density s to the cube of FO temperature ratio, $s/T^3 \simeq 7$ [10, 11], is robust [1], if the realistic particle table with the hadron masses up to 2.5 GeV is used and the hard-core hadronic repulsion is included. This is clearly seen by comparing the right panel of Fig. 1 with both panels of Fig. 2. At the same time in [1] it was shown that despite an essential difference with the approach used in [5], the both versions of the hadron resonance gas model demonstrate almost the same value 7.18 for the entropy per particle at chemical FO. In other words, the criterion of adiabatic chemical FO is, indeed, the robust one.

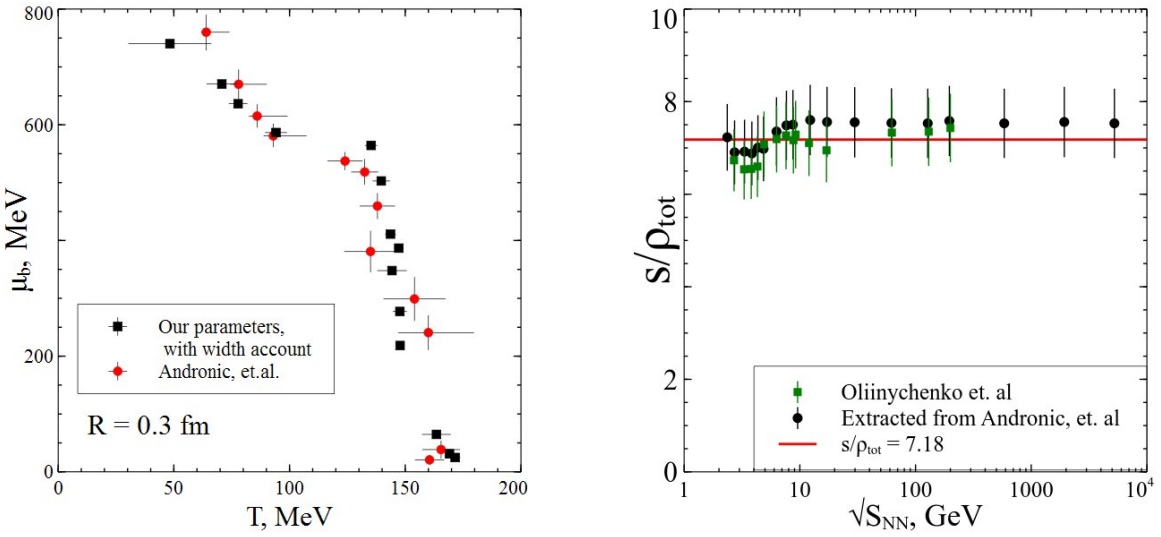

Figure 1: Comparison of the chemical FO parameters of HRGM1 [5] and HRGM2 [1]. **Left panel:** baryonic chemical potential vs. the chemical FO temperature for HRGM1 (circles) and HRGM2 (squares). **Right panel:** entropy per particle at chemical freeze-out $s/\rho \simeq 7.18$ vs. the center of mass energy per nucleon $\sqrt{s_{NN}}$. The shown errors are combined the statistical and systematic errors. The results of HRGM2 (squares) are very similar to that ones obtained by HRGM1.

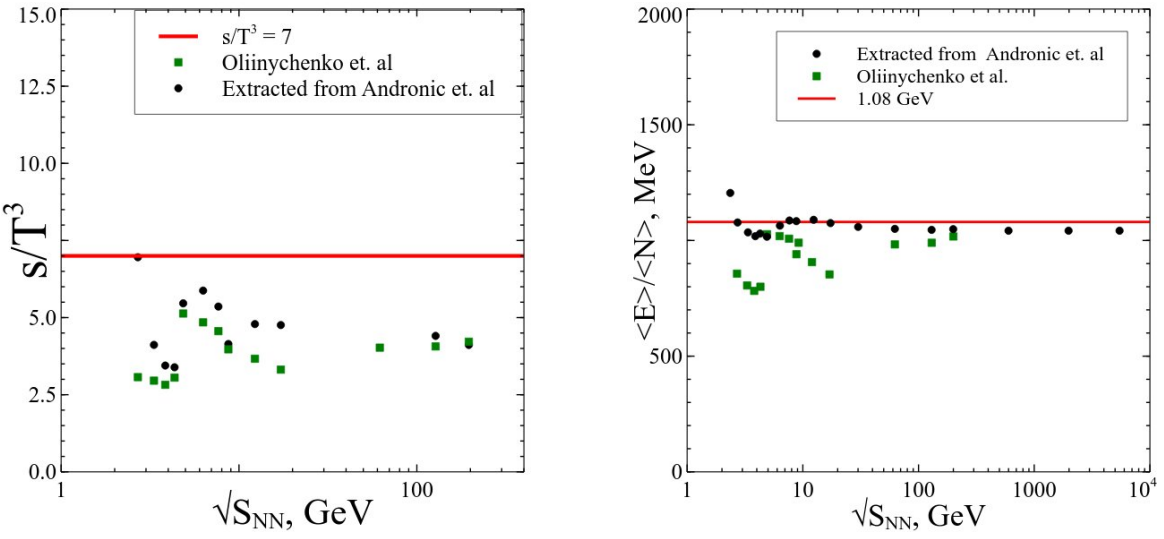

Figure 2: Different chemical freeze-out criteria. **Left panel:** ratio of the entropy density to the cube of temperature s/T^3 at chemical freeze-out vs. the center of mass energy $\sqrt{s_{NN}}$. Results of the HRGM1 (HRGM2) are shown by circles (squares). **Right panel**: energy per particle $\langle E\rangle/\langle N\rangle$ at chemical chemical freeze-out vs. $\sqrt{s_{NN}}$. Notations are the same as in the left panel.

A puzzle of the adiabatic chemical FO led us to a formulation of the model equation of state [3, 4]

$$p_M = C_M\ T^{A_M}\ \exp\left[-\frac{m_M}{T}\right], \quad p_B = C_B\ T^{A_B}\ \exp\left[\frac{\mu_B - M_B}{T}\right], \tag{1}$$

which successfully parameterizes the baryonic pressure p_B and the mesonic one p_M of the HRGM2. The pressure of antibaryons is also described by the right Eq. (1), but for negative value of the baryonic chemical potential extracted from the data at chemical FO, i.e. $\mu_{\bar{B}} = -\mu_B$. The constants $C_a,\ A_a,\ m_a$ with $a \in \{M, B\}$ in (1) parameterize the integrated hadronic mass spectrum and should be determined from the fit of the adiabatic chemical FO parameters. The remarkable fact, however, is that one can get rather good description of the constant entropy per particle by fitting only the mesonic and baryonic particle densities for which the mean deviations squared per degree of freedom, respectively, are $\chi^2_M/dof \simeq 0.42/11$ and $\chi^2_B/dof \simeq 7.8/11$. In other words, once the particle densities of the system (1) are reproduced, the corresponding entropy densities are automatically reproduced well giving the total mean deviation squared $\chi^2_{tot}/dof \simeq 19.4/36$. The latter includes the sum of mean deviations squared of meson density together with the one of baryons and their full entropy per particle at chemical FO.

The system (1) is a further refinement of the original E. Shuryak idea proposed for vanishing baryonic densities [12] and the found powers $A_B \simeq 6.097 \pm 0.38$ and $A_M \simeq 5.31 \pm 0.14$ are very close to the early estimate of Ref. [12]. Additionally, under the well justified assumptions the present model allows us to uniquely determine an effective density of states of hadronic mass spectrum using the inverse Laplace technic [3]. The found density of baryonic states is $\frac{\partial \varrho_B(m)}{\partial m} \sim \frac{(m-M_B)^{A_B-3.5}}{m^{\frac{3}{2}}}$, while the mesonic one is $\frac{\partial \varrho_M(m)}{\partial m} \sim m^{A_M-4}$, i.e. these densities of states are power-like rather than the exponential one. Moreover, numerical estimates show that for hadronic masses below 2.5 GeV these densities of states essentially differ from the empirical power-like hadronic density of states $\frac{\partial \varrho^{emp}(m)}{\partial m} \simeq \frac{4.11}{470\,\mathrm{MeV}} \left[\frac{m}{470\,\mathrm{MeV}}\right]^{3.11}$ found in [13] from the Particle Data Group [14] data. Our searches for possible reasons of such a difference led to a discovery of two new effects based on the modification of the wide resonance (and quark gluon bag) properties in a thermal medium [3, 4].

3. Thermal enhancement and sharpening of wide resonances at chemical FO. In order to demonstrate these new effects, here we consider the Gaussian mass attenuation of wide resonances instead of the Breit-Wigner one that is used in the actual simulations, since in this case the evaluation is more transparent. Such a treatment gives only about 10 % difference from the Breit-Wigner one [4], but it also allows us to obtain some important conclusions on the mass spectrum of quark-gluon (QG) bags which according to [15, 16] should unavoidably have the Gaussian mass attenuation. Note that such an estimate provide us with the lower limit, since the Gaussian mass distribution vanishes much faster than the Breit-Wigner one. The typical term of the k-resonance that enters into the mass spectrum of the hadron resonance gas model is given by $F_k(\sigma_k) \exp\left[\frac{\mu_k}{T}\right]$ [1, 5] (here μ_k is the chemical potential of this resonance) with

$$F_k(\sigma_k) \ \equiv \ g_k \int\limits_0^\infty dm\, \frac{\Theta\left(m - M_k^{Th}\right)}{N_k(M_k^{Th})}\, \exp\left[-\frac{(m_k - m)^2}{2\,\sigma_k^2}\right] \int \frac{d^3p}{(2\pi\hbar)^3} \exp\left[-\frac{\sqrt{p^2+m^2}}{T}\right]. \tag{2}$$

Here m_k is the mean mass of the k-th resonance, g_k is its degeneracy factor, σ_k is the Gaussian width which is related to the true resonance width as $\Gamma_k = Q\,\sigma_k$ (with $Q \equiv 2\sqrt{2\,\ln 2}$) and the normalization factor is defined via the threshold mass M_k^{Th} of the dominant channel as $N_k(M_k^{Th}) \equiv \int\limits_{M_k^{Th}}^\infty dm\ \exp\left[-\frac{(m_k-m)^2}{2\,\sigma_k^2}\right]$. For the narrow resonances the term $F_k(\sigma_k)$ converts into the usual thermal

density of particles, i.e. for $\sigma_k \to 0$ one has $F_k \to g_k\,\phi(m_k,T)$, where the following notation is used $\phi(m,T) \equiv \int \frac{d^3p}{(2\pi\hbar)^3} \exp\left[-\frac{\sqrt{p^2+m^2}}{T}\right]$. The momentum integral in (2) can be written using the non-relativistic approximation $\phi(m,T) \simeq \left[\frac{m\,T}{2\,\pi\,\hbar^2}\right]^{\frac{3}{2}} \exp\left[-\frac{m}{T}\right]$. Then to simplify the mass integration of (2) one can make the full square in it from the powers of $(m_k - m)$ and get

$$F_k(\sigma_k) \;\equiv\; g_k \int\limits_0^\infty dm\, f_k(m) \simeq \tilde{g}_k \int\limits_0^\infty dm\, \frac{\Theta\left(m - M_k^{Th}\right)}{N_k(M_k^{Th})} \exp\left[-\frac{(\tilde{m}_k - m)^2}{2\,\sigma_k^2}\right] \left[\frac{m\,T}{2\pi\hbar^2}\right]^{\frac{3}{2}} \exp\left[-\frac{m_k}{T}\right], \quad (3)$$

where an effective resonance degeneracy $\tilde{g}_k$ and an effective resonance mass $\tilde{m}_k$ are defined as

$$\tilde{g}_k \;\equiv\; g_k \exp\left[\frac{\sigma_k^2}{2\,T^2}\right] = g_k \exp\left[\frac{\Gamma_k^2}{2\,Q^2\,T^2}\right], \quad \tilde{m}_k \equiv m_k - \frac{\sigma_k^2}{T} = m_k - \frac{\Gamma_k^2}{Q^2\,T}\,. \quad (4)$$

From Eq. (4) one can see that the presence of the width, firstly, may strongly modify the degeneracy factor g_k and, secondly, it may essentially shift the maximum of the mass attenuation towards the threshold or even below it. There are two corresponding effects which we named as *the near threshold thermal resonance enhancement* and *the near threshold resonance sharpening*. These effects formally appear due to the same reason as the famous Gamow window for the thermonuclear reactions in stars [17]: just above the resonance decay threshold the integrand $f_k(m)$ in (3) is a product of two functions of a virtual resonance mass m, namely, the Gaussian attenuation is an increasing function of m, while the Boltzmann exponent strongly decreases above the threshold. The resulting attenuation of their product has a maximum, whose shape, in contrast to the usual Gamow window, may be extremely asymmetric due to a threshold presence. Indeed, as one can see from the left panel of Fig. 3 the resulting mass attenuation of a resonance may acquire the form of the sharp and narrow peak that closely resembles an icy slide.

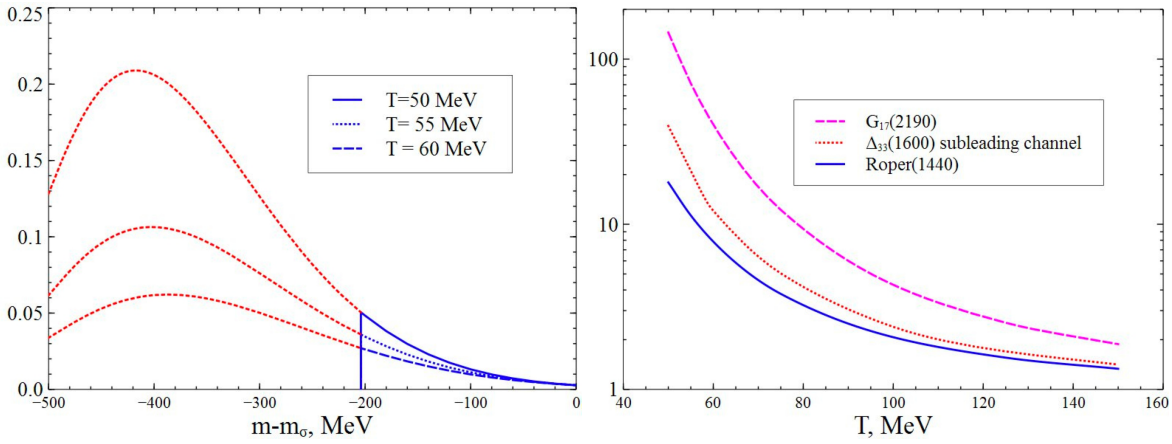

Figure 3: **Left panel:** Typical temperature dependence of the mass distribution $f_\sigma(m)/\phi(m_\sigma,T)$ (in units of 1/MeV, see Eq. (3)) for σ-meson with the mass $m_\sigma = 484$ MeV, the width $\Gamma_\sigma = 510$ MeV [18] and two pion threshold $M_\sigma^{Th} = 2\,m_\pi \simeq 280$ MeV. In the left panel the short dashed curves demonstrate that at these temperatures the maximum of the full mass distribution is shifted well below the two pion threshold (vertical line at $m - m_\sigma = -204$ MeV) and, hence, the resulting effective mass attenuation of a wide resonance acquires an icy slide shape. **Right panel:** Typical temperature dependence of the resonance enhancement. The ratio $R(T) = \frac{F_k}{g_k\,\phi(m_k,T)}$ is shown for a few hadronic resonance decays. For wide resonances the effect of enhancement can be huge.

To our best knowledge a special attention to the thermal enhancement of the $\Delta_{33}(1232)$ isobar in a thermal medium was for the first time paid in [19], although no detailed explanation of this effect

was given in [19]. The mass shift and shape modification of ρ meson in a hot hadronic matter were found in [20]. However, in both cases the found effects were not very strong since the considered resonances are not really wide. An analysis of the wide resonances' modification performed in [3, 4] gave the astonishing results. From the effective resonance degeneracy $\tilde{g}_k$ and the effective resonance mass $\tilde{m}_k$ defined in (4) one can see that they essentially differ from their vacuum values for $T \ll \sigma_k$. The left panel of Fig. 3 demonstrates a strong modification of the σ-meson mass attenuation at low temperatures which leads to the near threshold resonance sharpening. A simple analysis shows that the effect of resonance sharpening is strongest, if the threshold mass is shifted above the convex part of the Gaussian distribution in (3), i.e. for $M_k^{Th} \geq \tilde{m}_k$ or for the temperatures T well below $T_k^+ \equiv \frac{\sigma_k^2}{m_k - M_k^{Th}}$. In this case near the threshold a resonance acquires a narrow effective width [3, 4]

$$\Gamma_k^N(T) \simeq \frac{\ln(2)}{\frac{1}{T} - \frac{1}{T_k^+}} . \tag{5}$$

The right panel of Fig. 3 shows that an effect of near threshold enhancement compared to the thermal particle density of the same resonance taken with a vanishing width can be, indeed, huge for wide ($\Gamma \geq 450$ MeV) and medium wide ($\Gamma \simeq 300-400$ MeV) resonances. This effect can naturally explain the strong temperature dependence of hadronic pressure (1) at chemical FO, which in its turn generates the discussed power-like mass spectrum of hadrons. The other important conclusion from this analysis is that there is no sense to discuss the mass spectrum of hadronic resonances, empirical or Hagedorn, without a treatment of their width. Furthermore, the same is true for the QG bags which, according to the finite width model [15, 16], are heavy and wide resonances having the mass M_B larger than $M_0 \simeq 2.5$ GeV and the mean width of the form $\Gamma_B \simeq \Gamma_0(T) \left[\frac{M_B}{M_0}\right]^{\frac{1}{2}}$. Here $\Gamma_0(T)$ is a monotonically increasing function of temperature T and $\Gamma_0(0) \in [400; 600]$ MeV [15, 16].

The estimates of [3, 4] based on the finite width model and the approach outlined above show that our best hopes to find the QG bags experimentally may be related to their sharpening and enhancement by a thermal medium. Then at the chemical FO temperatures of about $T \simeq 80 - 140$ MeV the *QG bags may appear directly or in decays as narrow resonances with the width of about 50-150 MeV which have the mass about or above 2.5 GeV and which are absent in the tables of elementary particles.* Note that this range of chemical FO temperatures correspond to the center of mass energy of collision $\sqrt{s_{NN}} \in [4; 8]$ GeV [1, 5], which is in the range of the NICA JING and FAIR GSI energies of collision. This energy range sets the most promising kinematic limit for the QG bag searches.

4. Strangeness Horn description and chemical FO of strange particles. A novel feature of principal importance implemented into the HRGM2 [1, 2] is its multicomponent hard-core repulsion. One of the traditional difficulties of the HRGM was related to the Strangeness Horn description which up to recently was far from being satisfactory, although very different versions of the HRGM were used for this purpose (see [2] for a discussion and references). The HRGM2 with the multicomponent hard-core repulsion allows one to describe the hadron yield ratios from the low AGS to the highest RHIC energies. In [2] it was demonstrated that the variation of the hard-core radii of pions and kaons leads to a drastic improvement of the fit quality of the measured mid-rapidity data and for the first time such a model provides us with a complete description of the Strangeness Horn behavior as the function of the energy of collision without spoiling the fit quality of other ratios. The best global fit with $\chi^2/dof = 80.5/69 \simeq 1.16$ is found for an almost vanishing hard-core radius of pions of 0.1 fm and for the hard-core radius of kaons being equal to 0.38 fm, whereas the hard-core radius of all other mesons is found to be 0.4 fm and that one of baryons is equal to 0.2 fm. Fig. 4 demonstrates that within the multicomponent HRGM2 the mean deviation squared per data is $\chi^2/dof \simeq 7.5/14$ for K^+/π^+ and $\chi^2/dof \simeq 14/12$ for Λ/π^- ratios. Note that

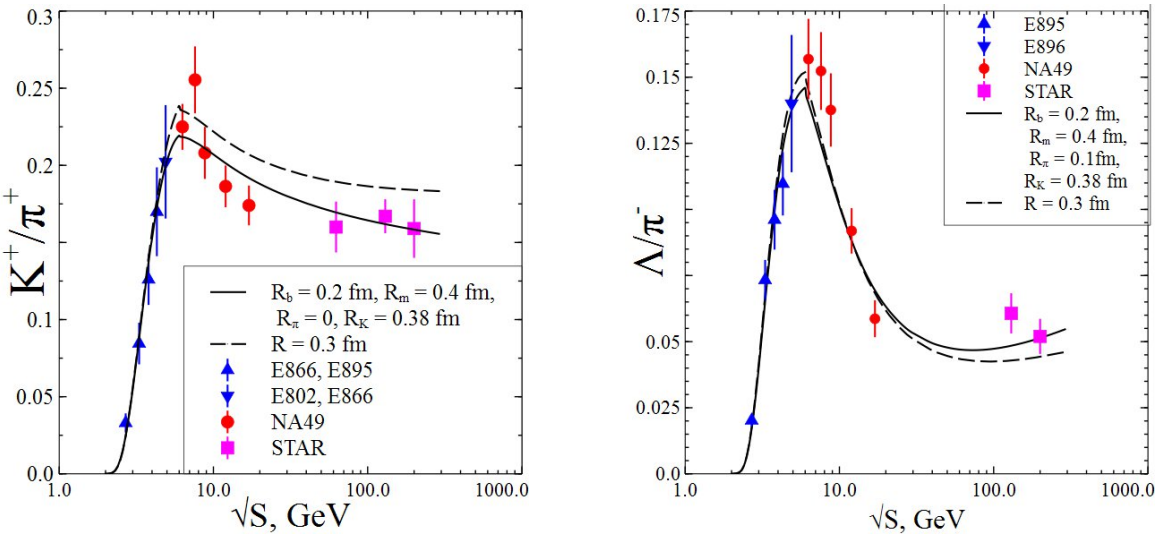

Figure 4: $\sqrt{s_{NN}}$ dependences of K^+/π^+ (left panel) and Λ/π^- (right panel) ratios obtained in [2] within the multicomponent model are compared to that ones found within the one-component model [1].

the value of χ^2/dof obtained for K^+/π^+ ratio is almost three times smaller compared to the best fit of the one-component model.

Note, however, that in order to demonstrate its new abilities the strangeness suppression factor γ_s [21, 22] in the multicomponent HRGM2 [2] simulations was kept to be a unity. In the most recent version of the HRGM2 [23] we fixed the hard-core radii values found earlier and included γ_s into the fitting procedure. The obtained results have a better fit quality $\chi^2/dof = 63.4/55 \simeq 1.15$ for all 14 energies of collision in the range from the low AGS to the highest RHIC energies. As one can see from the upper left panel of Fig. 5 the γ_s fit greatly improves the K^+/π^+ ratio allowing us to correctly reproduce even the peak of the Strangeness Horn! From the lower panels of this figure one, however, can deduce that the γ_s fit does not allow us to improve the description of the ratios of antihyperon-hyperon with nonzero strangeness, i.e. $\bar{\Lambda}/\Lambda$, $\bar{\Xi}/\Xi$ and $\bar{\Omega}/\Omega$. Also the antiproton to pion ratio is almost not improved by this fit. Moreover, the γ_s fit does not improve any ratios at $\sqrt{s_{NN}} \simeq 17$ GeV (see the lower right panel in Fig. 5)!

In order to get rid of the phenomenological parameter γ_s and to further improve the fit quality of hadron multiplicities, we worked out an alternative concept of the strange particles chemical FO (SPFO) [23]. Its main assumption is that the SPFO occurs separately from the chemical FO of nonstrange hadrons (UDFO hereafter). A partial justification for such a hypothesis is given in [24, 25, 26], where the early chemical and kinetic FO of Ω hyperons and J/ψ mesons is discussed for the energies above the highest SPS energy.

A similar idea of separate chemical FO of strange particles was suggested in [27]. However, in contrast of ideal gas treatment of [27], our SPFO concept accounts for conservation laws connected the UDFO and the SPFO. To determine the SPFO baryonic chemical potential, the chemical potential for a third projection of isospin and strange chemical potential we employ an isentropic evolution of the system between the UDFO and the SPFO, and the conservation laws of baryonic charge, third projection of isospin and strangeness. Therefore, the SPFO concept has only one additional fitting parameter, the SPFO temperature, compared to the HRGM2 [2] and, hence, the number of its independent degrees of freedom coincides with the one for the γ_s fit.

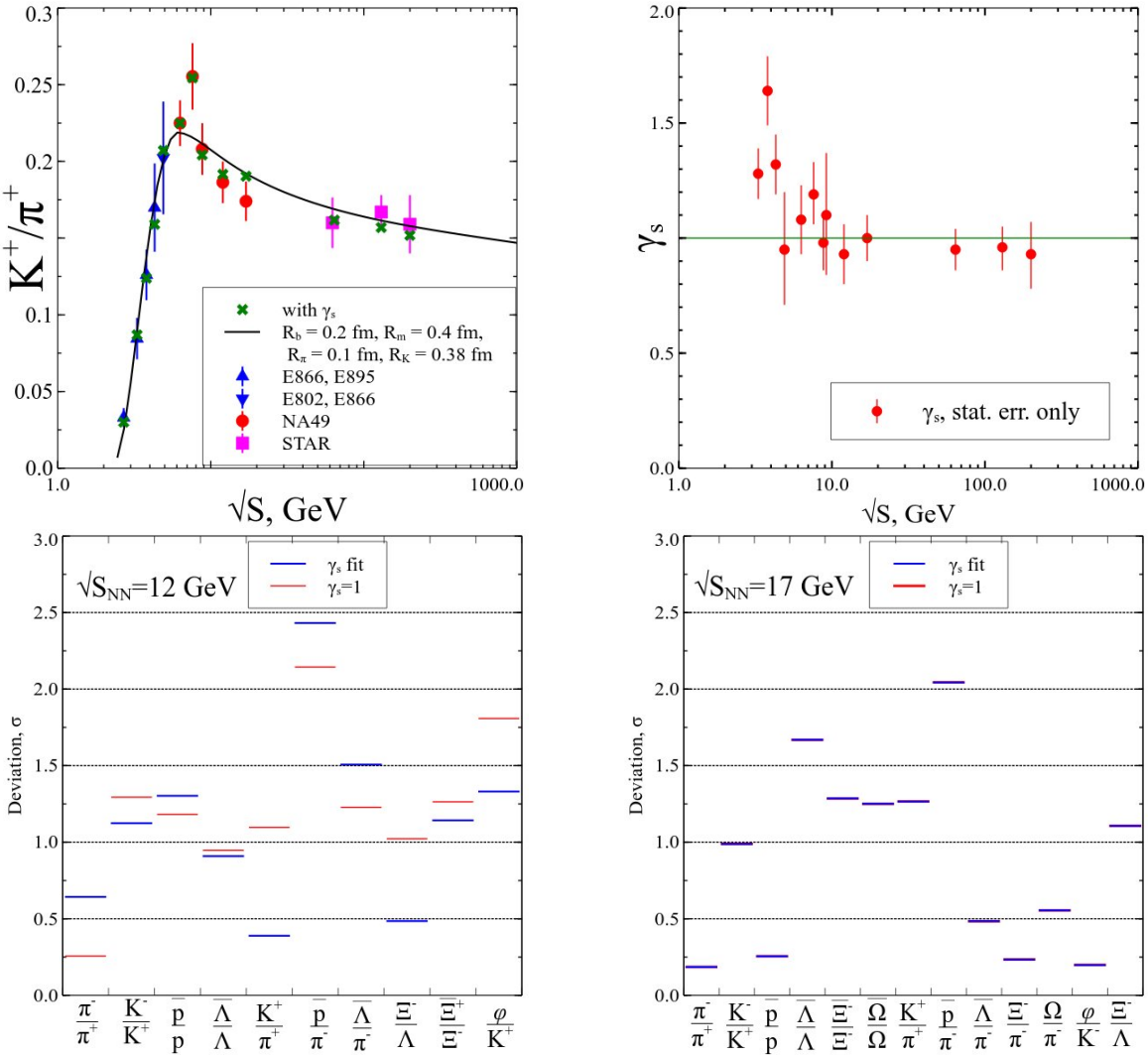

Figure 5: **Upper left panel:** $\sqrt{s_{NN}}$ dependence of K^+/π^+ ratio for γ_s included into the fit (crosses) and for $\gamma_s = 1$ (solid curve) [2]. **Upper right panel:** $\sqrt{s_{NN}}$ dependence of γ_s obtained from the new fit shown in the left panel. **Lower panels:** Comparison of the relative deviations of the fit results from experimental ratios is shown for $\sqrt{s_{NN}} \simeq 12$ GeV (left) and $\sqrt{s_{NN}} \simeq 17$ GeV (right).

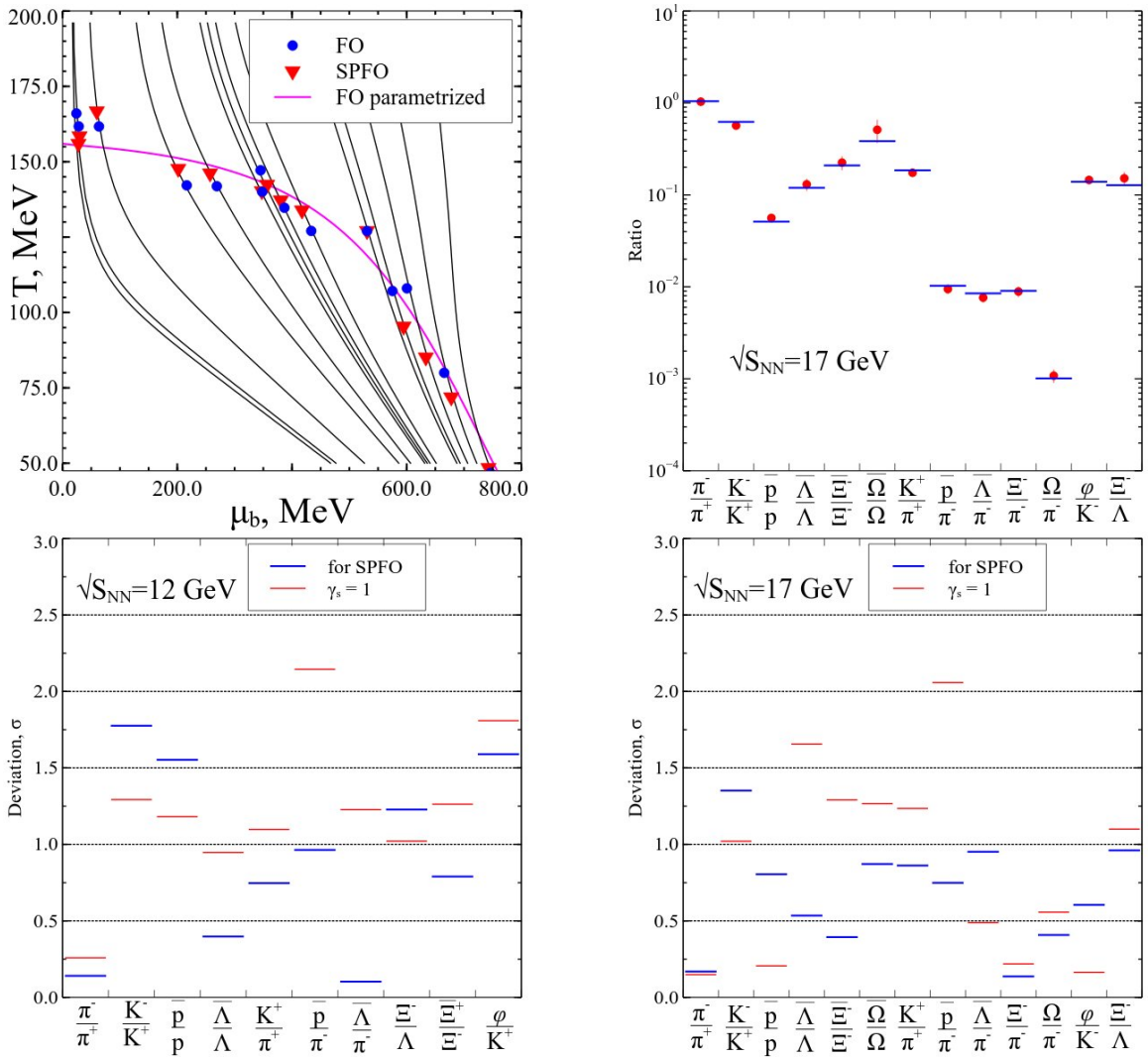

Figure 6: **Upper left panel:** μ_b and T values for UDFO (circles) and SPFO (triangles) are shown along with their isentropic trajectories (thin curves). **Upper right panel:** Example of the ratios description within the SPFO approach for $\sqrt{s_{NN}} \simeq 17$ GeV. **Lower panels:** Same as in the lower panels of Fig. 5, but for the SPFO approach.

The ratio of hadron $p1$ multiplicity to hadron $p2$ multiplicity is defined as

$$\frac{n_{p1}^{final}}{n_{p2}^{final}} = \frac{\sum_X n_X^{therm}(SPFO)Br(X \to p1)\frac{V_{SPFO}}{V_{UDFO}} + \sum_Y n_Y^{therm}(UDFO)Br(Y \to p1)}{\sum_X n_X^{therm}(SPFO)Br(X \to p2)\frac{V_{SPFO}}{V_{UDFO}} + \sum_Y n_Y^{therm}(UDFO)Br(Y \to p2)}\,, \tag{6}$$

where the UDFO and SPFO 'volumes' (in fact, the corresponding hypersurface extents) are related via the baryonic n_B and isospin n_{I3} densities as $\frac{V_{SPFO}}{V_{UDFO}} = \frac{n_B^{UDFO}}{n_B^{SPFO}} = \frac{n_{I3}^{UDFO}}{n_{I3}^{SPFO}}$ due to conservation laws discussed above. The sums in Eq. (6) run over over all hadronic species including $p1$ and $p2$. In the latter case the corresponding branching ratios of decay are defined as $Br(p1 \to p1) = 1$ and $Br(p2 \to p2) = 1$, whereas for $X \neq p$ the branching ratios of decay $Br(X \to p)$ are taken from the Particle Data Group [14]. Due to the conservation laws an effective number of degrees of freedom in the SPFO approach is the same as in case of the γ_s fit, but the fit quality is better $\chi^2/dof = 58.5/55 \simeq 1.06$ than for the γ_s fit. As one can see from Fig. 6, the fit of particle ratios which were problematic for the γ_s fit gets better, but not at an expense of an essential worsening of other ratios. Therefore, *the SPFO concept [23], outlined here, provides us with more realistic and reliable approach, then a popular concept of strange suppression factor* γ_s.

5. Conclusions. In this work we discussed the new results obtained within the multicomponent version of the HRGM2. This model allowed us to demonstrate that the most robust criterion of chemical FO is the adiabatic FO criterion of constant entropy per particle equal to 7.18. Searches for a physical explanation of this phenomenon, led us to a thorough analysis of effective hadronic mass spectrum. One of the most important conclusions of our studies is that the width of resonances and QG bags should unavoidably be included into statistical models and, hence, there is no sense to discuss the hadronic mass spectrum, empirical or Hagedorn, without accounting for the width of constituents. Moreover, we showed that the properties of wide resonances are essentially modified at chemical FO. Using the effect of near threshold resonance sharpening, we argued that, if the QG bags are formed in heavy ion collisions, then in experiments they may appear directly or in decays as narrow and heavy resonances with the width about 50-150 MeV which are absent in the tables of elementary particles. Our estimates show that such resonances may appear at the chemical FO temperatures of about $T \simeq 80 - 140$ MeV which corresponds to $\sqrt{s_{NN}} \in [4; 8]$ GeV. This range of the center of mass energy of collision exactly fits into the NICA and FAIR Projects.

Also we demonstrated that the HRGM2 with the multicomponent hard-core repulsion is able to drastically improve the description of K^+/π^+ and Λ/π^- ratios which were problematic for other formulations of HRGM. The most recent development of the HRGM2 includes a novel concept of the SPFO, which seems to be physically more adequate for a description of the strange hadron multiplicity ratios than the popular strangeness suppression factor approach. Therefore, one of the future physical tasks will be to find a physical reason of why the chemical FO of strange particles at $\sqrt{s_{NN}} < 5$ GeV occurs at lower temperatures than the FO of hadrons built up from u and d quarks, and why it is vise versa for $\sqrt{s_{NN}} > 9$ GeV.

All versions of the HRGM2 discussed here show that in a narrow range of collision energy $\sqrt{s_{NN}} \in [4.3; 4.9]$ GeV there exist some peculiar irregularities in a behavior of the chemical FO temperature, in entropy density and in total particle number density. From the left panel of Fig. 1 it is seen that about 15 % increase of $\sqrt{s_{NN}}$ leads to about 10 % change of the baryonic chemical potential μ_B, whereas the chemical FO temperature increases by a factor 1.5. From the left panel of Fig. 2 one can also see a simultaneous appearance of irregularity for s/T^3 ratio which jumps over 2 times, leading to 6.75 times resulting increase of entropy density while $\sqrt{s_{NN}}$ increases by about 15 % only! Moreover, due to the adiabatic chemical FO such a small variation of collision energy leads to about 6.75 times increase of the particle density, while the chemical FO 'volume' changes on about 20 % [1] only! Note that all these irregularities can be naturally explained within the shock adiabat

model of central nuclear collisions [28, 29] as a formation of the mixed quark-gluon-hadron phase. However, to safely reveal the physical cause of all discussed phenomena occurring at the collision energy interval $\sqrt{s_{NN}} \in [4.3; 4.9]$ GeV and to elucidate their relation to the irregularities observed at slightly higher collision energy $\sqrt{s_{NN}} \simeq 7.6$ GeV, we need an accelerator of new generation working in this energy range with much higher experimental accuracy. It seems that the NICA JINR and FAIR GSI Projects are perfectly suited to resolve these tasks.

Acknowledgments. The authors are thankful to D. B. Blaschke and A. S. Sorin for important comments. The fruitful discussions with S. V. Molodtsov, D. H. Rischke and E. V. Shuryak are acknowledged. This publication is based on the research provided by the grant support of the State Fund for Fundamental Research (project N Φ58/175-2014).

References

[1] D.R. Oliinychenko, K.A. Bugaev and A.S. Sorin, Ukr. J. Phys. **58**, 211 (2013).

[2] K. A. Bugaev, D. R. Oliinychenko, A. S. Sorin, G. M. Zinovjev, Eur. Phys. J. A **49**, (2013) 30.

[3] K. A. Bugaev, D. R. Oliinychenko, E. G. Nikonov, A. S. Sorin and G. M. Zinovjev, PoS Baldin ISHEPP XXI (2012) 017, 1-14; arXiv:1212.0132 [hep-ph].

[4] K. A. Bugaev, A. I. Ivanytskyi, D. R. Oliinychenko, E. G. Nikonov, V. V. Sagun and G. M. Zinovjev, arXiv:1312.4367 [hep-ph].

[5] A. Andronic, P. Braun-Munzinger and J. Stachel, Nucl. Phys. A **772**, 167 (2006).

[6] A. Andronic, P. Braun-Munzinger and J. Stachel, Phys. Lett. B **673**, 142 (2009) and references therein.

[7] J. Cleymans, H. Oeschler, K. Redlich, and S. Wheaton, Phys. Rev. C 73, 034905 (2006).

[8] J. Cleymans, K. Redlich, Phys. Rev. Lett. **81**, 5284 (1998).

[9] J. Cleymans, K. Redlich, Phys. Rev. C 61 054908 (1999).

[10] A. Tawfik, Europhys. Lett. **75**, 420 (2006).

[11] A. Tawfik, Nucl. Phys. A **764**, 387 (2006).

[12] E. V. Shuryak, Sov. J. Nucl. Phys. **16**, 220 (1973).

[13] T. D. Cohen and V. Krejcirik, J. Phys. G **39**, 055001 (2012).

[14] C. Amsler *et al.*, Phys. Lett. B **667**, 1 (2008) [http://pdg.lbl.gov].

[15] K.A. Bugaev, V.K. Petrov and G.M. Zinovjev, Europhys. Lett. **85**, 22002 (2009).

[16] K. A. Bugaev, V. K. Petrov and G. M. Zinovjev, Phys. Rev. **C 79**, (2009) 054913.

[17] C. S. Rolfs and W. S. Rodney, *Cauldrons in the Cosmos*, University of Chicago Press, 1986.

[18] R. Garcia-Martin, J. R. Pelaez and F. J. Yndurain, Phys. Rev. D **76**, 074034 (2007).

[19] K. G. Denisenko and St. Mrowczynski, Phys. Rev. C **35**, 1932 (1987).

[20] H.W. Barz *et al.*, Phys. Lett. B **265**, 219 (1991).

[21] F. Becattini *et al.*, Phys. Rev. C **69**, 024905 (2004).

[22] J. Letessier, J. Rafelski, nucl-th/0504028.

[23] K. A. Bugaev *et al.*, Europhys. Lett. **104** 22002 (2013).

[24] K. A. Bugaev, J. Phys. G **28**, 1981 (2002).

[25] M. I. Gorenstein, K. A. Bugaev and M. Gazdzicki, Phys. Rev. Lett. **88**, 132301 (2002).

[26] K. A. Bugaev, M. Gazdzicki, M. I. Gorenstein, Phys. Lett. B **544**, 127 (2002).

[27] S. Chatterjee, R.M. Godbole, S. Gupta, Phys. Lett. B, **727**, 554 (2013).

[28] K. A. Bugaev, A. I. Ivanytskyi, D. R. Oliinychenko, V. V. Sagun, I. N. Mishustin, D. H. Rischke, L. M. Satarov and G. M. Zinovjev, arXiv:1405.3575 [hep-ph].

[29] K. A. Bugaev, A. I. Ivanytskyi, D. R. Oliinychenko, V. V. Sagun, I. N. Mishustin, D. H. Rischke, L. M. Satarov and G. M. Zinovjev, arXiv:1412.0718 [nucl-th].